Journal of Structural Geology, Vol. 14, No. 8/9, pp. 999 to 1006, 1992
Printed in Great Britain

0191-8141/92 $05.00+0.00

An argument against the crush origin of pseudotachylytes based on the analysis of clast-size distribution

TOSHIHIKO SHIMAMOTO

Earthquake Research Institute, University of Tokyo, 1-1-1 Yayoi, Bunkyo-ku, Tokyo 113, Japan

and

HIROYUKI NAGAHAMA

Institute of Geosciences, School of Science, Shizuoka University, 836 Ohya, Shizuoka 422, Japan

(*Received* 6 *September* 1991; *accepted in revised form* 5 *April* 1992)

Abstract—The origin of pseudotachylytes has been controversial since Wenk cast doubt on the melt origin of the matrix of pseudotachylytes, in 1978. The matrix of this rock is so fine grained that the crush origin of pseudotachylytes, revived by Wenk, cannot easily be denied. This paper presents a new line of argument based on the size analysis of clasts contained in pseudotachylytes in felsic granulite from the Musgrave Range, central Australia. These clasts are definitely crush products produced during the pseudotachylyte generation. Their sizes, as measured on photomicrographs of thin sections, obey the size distribution: $N = N'r^{-D}$, where N is the cumulative number of clasts with sizes greater than r, D is the fractal dimension, and N' is a constant that depends on the number of measurements. D was found to be 1.5 ± 0.05 for the size ranges of 10–2000 μm. If the matrix of the pseudotachylytes consists mostly of ultrafine crush products, they must have formed simultaneously with those coarse crush products. The proportion of fine products relative to the coarse clasts can be estimated, assuming that a similar size distribution also holds for the fine products. The estimated area occupied by fine products in a thin section is of the order of only several percent, whereas the measured area of the matix is about 60%. Thus the major part of the matrix of the pseudotachylytes cannot be regarded as crush products. It is also shown that the number of clasts smaller than about 5 μm becomes very small, perhaps as a result of nearly complete dissolution of fine clasts in a melt. However, if the ultrafine-grained matrix of the pseudotachylytes had formed by crushing during seismogenic fault motion, the grain-size refinement during the crushing should have occurred jumping the size range of at least 1–5 μm. This is quite unreasonable and disproves the crush origin for the matrix of pseudotachylytes.

INTRODUCTION

PSEUDOTACHYLYTES comprise an ultrafine-grained and generally dark-colored matrix containing various sizes of cataclastically deformed clasts, and they occur as veins or as networks with complex geometry (Philpotts 1964, Sibson 1975, among many others). The matrix of this rock is so fine grained that its origin has been controversial. A common interpretation is that the matrix of pseudotachylytes associated with faults formed as a result of frictional melting during seismogenic fault motion (Shand 1916, Sibson 1975). Wenk (1978), on the other hand, showed through TEM observation that the matrix of pseudotachylytes from a few localities is nearly free from glass and exhibits cold-worked microstructures such as tangled dislocations, and so he revived the 'flinty crush' (cataclasis) origin of Clough (1888). Weiss & Wenk (1983) later conducted violent experiments using a solid-pressure medium apparatus in which they successfully produced networks of finely comminuted fragments in severely fractured gabbro. Maddock (1983) opposed Wenk's interpretation and favored the melt origin of the matrix of pseudotachylytes based on microstructural evidence, such as the development of spherulitic and dendritic crystals, that are typical of rapid growth from a quenching melt, and on the disequilibrium chemistry of feldspar microlites.

One of the most important implications of the studies of pseudotachylytes is that the shear stress along faults can be estimated from the amount of pseudotachylyte generated per given fault displacement, as demonstrated by Sibson (1975). The stress along faults (not the stress drop during an earthquake) is closely related to the strength of the lithosphere, and hence the study of pseudotachylytes is linked to the state-of-stress problem (e.g. Hanks & Raleigh 1980) which is of major significance in the Earth Sciences. Sibson's estimation is valid only if the melt origin is correct. If instead the matrix of pseudotachylytes consists mostly of crush products, one must know the relationship between the work done during the frictional slip and the amount and characteristics of comminuted materials in order to estimate the stress from the same data. Unfortunately, such a relationship is poorly understood at present.

Despite its significance, confirmation of the origin of the matrix of pseudotachylytes is not simple. Mineral grains with tangled dislocations, such as those described by Wenk (1978), certainly cannot form during crystallization from melt. However, pseudotachylyte veins, especially those along large-scale faults, are likely to have undergone numerous seismogenic events after their for-

mation due to repeated fault motion. Thus it is difficult to distinguish the dislocations of later origin from initial ones. Some textural and chemical evidence, the latter in particular, can show convincingly a melt origin for at least part of the matrix of pseudotachylytes. For instance, Toyoshima (1990) reports pyroxene microlites in pseudotachylyte veins from south-central Hokkaido, Japan, that formed under the metamorphic condition of prehnite–pumpellyite facies. Such microlites cannot be regarded as the products of later devitrification or alteration, and hence they are most likely to have formed via crystallization from melt. But the major drawback of these approaches is that the spherulitic and dendritic crystals normally occupy only a small fraction of the matrix of pseudotachylytes. What then is the origin of the other part of the matrix? Microstructural and chemical evidence is not always unequivocal, because there exists a possibility that not all of the ultrafine-grained matrix of pseudotachylytes is of the melt origin.

We take a completely different approach here, based upon the analysis of the size distributioin of clasts contained in the matrix of a pseudotachylyte (Fig. 1). Okamoto & Kitamura (1990) have shown recently that the size distribution of clasts in a pseudotachylyte from the Outer Hebrides thrust zone in Scotland obeys a simple power law, as typically recognized for fragments fractured in various manners (e.g. Turcotte 1986). In essence, the power law indicates that the fraction of fragments of a certain range of size cannot form at random, but is uniquely related to the amount of fragments of other size ranges. Thus our basic idea was to examine whether or not the area occupied by the ultrafine-grained matrix of pseudotachylytes is consistent with the amount of submicroscopic fragments predicted from the measured size distribution of coarse-grained clasts. If they agree, the crush origin of the matrix of pseudotachylytes is viable; if they do not, the crush origin is not considered valid.

The main purpose of this paper is to propose a new method for such arguments in a self-contained manner. Here the method is applied only to an unusually thick pseudotachylyte from the Musgrave Range in central Australia (Moore & Goode 1978, Camachol & Vernon in preparation), for demonstrative purposes. Applications to other pseudotachylytes are now under way, and are so far giving similar results to those reported here and in Shimamoto & Nagahama (1991).

MEASUREMENTS OF CLAST SIZES

Samples for the analysis of clast-size distribution were collected from an eastern extension of the Woodroffe Thrust in the eastern Musgrave Range in central Australia (Fig. 1). At this location, the Precambrian felsic granulites were thrust over felsic mylonites to the north during Paleozoic time (Webb 1985). Amazingly, the pseudotachylyte-bearing zone is up to 1 km thick (Camachol & Vernon in preparation). The mylonites to the north change gradually from *S–C* mylonite into ultra-mylonite toward the pseudotachylyte-bearing zone. The granulite to the south does not exhibit pervasive mylonitic deformation.

A surprising feature of this thrust is that the pseudotachylyte-bearing zone is not observed to be accompanied by a pervasive cataclastic fault zone, despite the nearly perfect exposure. Pseudotachylyte veins (e.g. Figs. 1a & c) occur in a variety of complex modes, mixed with cataclastically deformed fragments of rocks and previously formed pseudotachylyte veins. Mylonitic deformation of pseudotachylytes is recognized very locally in the mylonite zone, but the mylonitic deformation is not at all predominant in the pseudotachylyte-bearing zone. Implications of those features will be discussed elsewhere.

Measurements of clast sizes were conducted on photomicrographs of the pseudotachylyte taken under plane-polarized light. The purpose of such measurements is to determine the size distribution of clasts with a wide range of sizes, that are scattered in the matrix of pseudotachylytes (Fig. 1d). Measurements of clasts over a wide area is essential to perform non-biased measurements for such a purpose. Thus the measurements were performed over an entire thin section using an optical microscope, rather than using SEM or TEM. The matrix of the pseudotachylyte is light to dark brown colored, whereas the quartz–feldspathic clasts appear white to colorless under plane polarized light. The sizes of clasts as small as 1–2 μm were measurable on the enlarged photomicrographs, due to this marked contrast in color between the clasts and the matrix.

To avoid biased measurements, the major and minor axes, A and B, were measured for all clasts on the photomicrographs, using a binocular lupe that can be mounted on the head. We first recorded the measured sizes directly onto a tape recorder while continuing measurements, and then later transferred the data onto a personal computer for automatic data processing. The use of a tape recorder greatly speeded up the measurements.

The results were plotted as cumulative frequency diagrams for the major axis, A, and for the mean diameter, r, defined as the geometric mean of A and B, using logarithmic scales on both axes (Fig. 2). The cumulative number N is the number of clasts whose sizes are greater than r or A. It is evident from Fig. 2 that linear relationships hold for log (N) vs log (r) plots and for log (N) vs log (A) plots. Hence, empirical power laws of the form:

$$N = N_A A^{-D_A} \tag{1}$$

and

$$N = N_r r^{-D_r} \tag{2}$$

hold at least for the size range of 10–2000 μm, where N_A and N_r are constants that depend on the number of measurements. D_A and D_r are called fractal dimensions with respect to the size distributions of the major axis and the mean diameter, respectively (simply called 'fractal dimensions' hereafter).

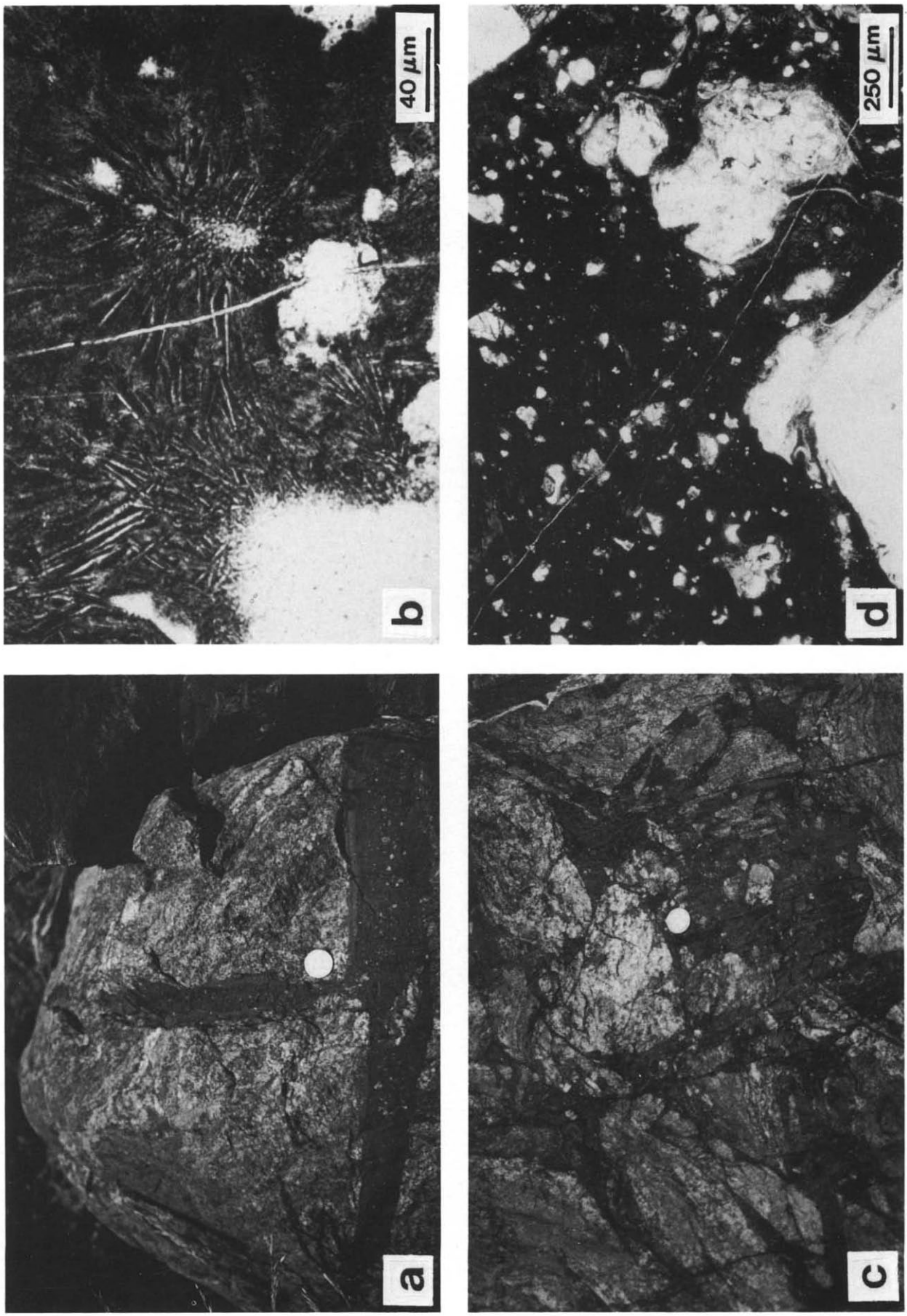

Fig. 1. Pseudotachylytes (PT) in felsic granulite from the Musgrave Range in central Australia. (a) PT veins injected into fractured granulite: note well-developed chilled margin. (b) A photomicrograph of PT under plane-polarized light, showing spherulitic plagioclase microlites surrounding plagioclase clasts with corroded margins. (c) A network of PT veins with cataclastically deformed rock fragments of various sizes. (d) A photomicrograph under plane-polarized light of quartzo-feldspathic clasts of various sizes. For scales, the coins in (a) and (c) are 25 mm in diameter.

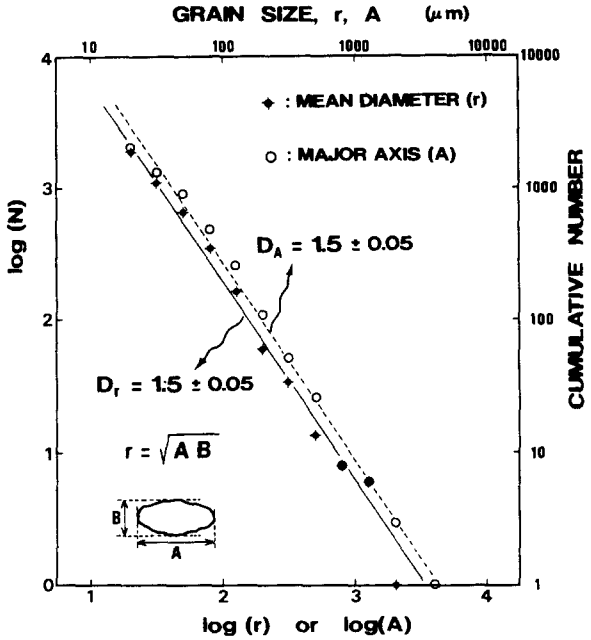

Fig. 2. Size distribution of clasts contained in the felsic pseudotachylyte (specimen No. 1) from the Musgrave Range, central Australia. A and B denote, respectively, the major and minor axes of clasts, and r is the geometric mean of A and B. N is the cumulative number of clasts whose mean diameter is greater than r (closed circles) or whose major axis is greater than A (open circles). D_r and D_A are fractal dimensions with respect to the size distributions of r and A, respectively, as determined by use of the least-squares method. The standard error for the fractal dimension is also given.

The fractal dimensions, D_A and D_r, are nearly identical (Fig. 2). This follows from the fact that the aspect ratio, A/B, or the shape of the clasts does not change systematically with the size of clasts (Fig. 3). To see this, denote the aspect ratio by R, which yields $\log(r) = \log(A) - \log(R)/2$. Thus one can simply obtain $\log(r)$ from $\log(A)$ by horizontally shifting the sizes, and this is what is recognized in Fig. 2. Later arguments will be made only in terms of r.

The frequency distribution of clasts in pseudotachylytes may appear to be random at a glance (Fig. 1d), but a surprisingly simple law actually holds as demonstrated first for the clasts in pseudotachylytes by Okamoto & Kitamura (1990).

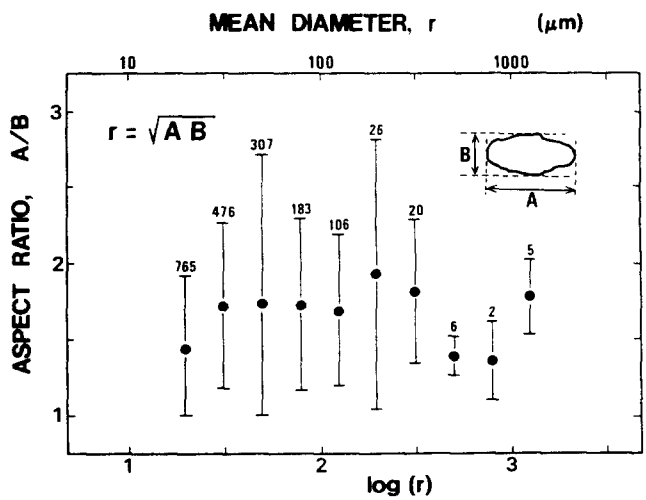

Fig. 3. Aspect ratio, A/B, plotted against the mean diameter, r, of the clasts in pseudotachylyte (specimen No. 1) from the Musgrave Range. Solid circles indicate the average aspect ratio in each size division on the log (r) axis. The vertical bars denote the double standard deviations around the mean value of r. Since the lower bound for r is 1 by definition, the lowest margin of the vertical bars is set to be 1. The small number on top of the vertical bar gives the number of measurements in each size division.

POWER-LAW SIZE DISTRIBUTION

Although still empirical, power laws have been used extensively to describe size distributions of a wide variety of fragmented objects (Gaudin 1926, Schuhmann 1960, Takeuchi & Mizutani 1968, Hartmann 1969, Fujiwara *et al.* 1977, Sammis *et al.* 1986, Turcotte 1986, Nagahama 1991, among many others; for broader mathematical background see Mandelbrot 1982, Schroeder 1991). We shall briefly summarize below some of the unique properties of the power-law size distribution for the sake of later arguments, using the derivation of the power law by Matsushita (1985).

Let us consider the size distribution only in terms of the cumulative number, $N(r)$, whose sizes are greater than a characteristic size, r. A simple case in which a power law holds is illustrated by a one-dimensional size distribution shown in Fig. 4(a). Consider a thin, long bar whose size is specified only by its length. A power-law size distribution can be created as follows.

Divide a bar with unit length into three bars and stipple one of them (CD in Fig. 4a). Then divide the remaining bars into three and stipple one of them (EF and GH in Fig. 4a). Divide the unstippled bars further

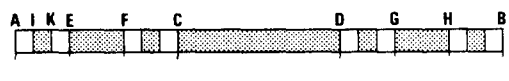

(a)

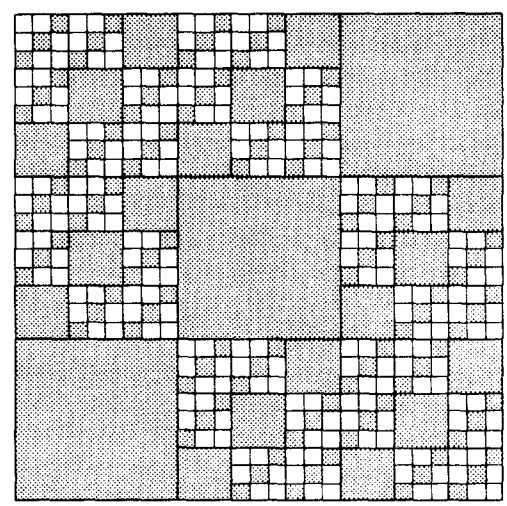

(b)

Fig. 4. (a) A 'middle-third erasing' Cantor set for which a power law with fractal dimension, D^1, of log 2/log 3 ≈ 0.63 holds. (b) Self-similarly arranged squares, which are equivalent to the Sierpinski carpet, with fractal dimension, D^2, of log 6/log 3 = 1.63. Note that D^2 is greater than D^1 by 1.

into three and stipple one in each group (e.g. IK). After the nth step, the length of the smallest bar is 3^{-n}, and the cumulative number of stippled bars is given by:

$$N(r) = 1 + 2 + 2^2 + 2^3 + \cdots + 2^{n-1} = 2^n - 1 \simeq 2^n. \quad (3)$$

Then the size and cumulative numbers satisfy the power law, and the fractal dimension in one dimension becomes:

$$D^1 = \log 2/\log 3 \simeq 0.63. \quad (4)$$

The actual fragmentation processes do not have to follow these steps. But in order for the power law to hold, fragmented objects must be such that the rearrangement such as that shown in Fig. 4(a) is possible. Note a self-similarity in Fig. 4(a); that is, AB is self-similar to AC and DB, which are similar to AE, FC, DG and HB. This self-similarity appears as long as the power law holds. Thus to use Schroeder's (1991) words, the power laws are "endless sources of self-similarity".

An equivalent two-dimensional set of objects can be constructed by arranging squares as shown in Fig. 4(b). In this case, a unit square is divided first into nine subsquares of the side of 1/3, and one square stippled on each row. Figure 4(b) can be obtained by repeating the same procedures to non-stippled squares twice more. After the nth step, the cumulative number of stippled squares with sides greater than 3^{-n} is given by:

$$N(r) = 3\{1 + (3^2 - 3) + (3^2 - 3)^2 + \cdots + (3^2 - 3)^{n-1}\} = 3(3^2 - 3)^n/5 - 3/5. \quad (5)$$

$N(r)$ is thus nearly proportional to $(3^2 - 3)^n$ when n is large ($n \gg 1$) and the two-dimensional fractal dimension is given by:

$$D^2 = \log (3^2 - 3)/\log 3 = \log 6/\log 3 \simeq 1.63. \quad (6)$$

Since the above fractal dimension is fairly close to that in Fig. 2, the clast size distribution in a pseudotachylyte from the Musgrave Range must be fairly similar to that in Fig. 4(b). Once again a self-similarity is obvious in Fig. 4(b). Note that the self-similarity in each row in Fig. 4(b) is equivalent to that of the one-dimensional set in Fig. 4(a). In such cases, $D^2 = D^1 + 1$ holds.

Matsushita (1985) derived a general equation for the d-dimensional fractal dimension:

$$D^d = \log (b^d - i)/\log b, \quad (7)$$

where unstippled hypercubes are subdivided into b^d equal-sized subcubes with the side reduced to $(1/b)$th of the side prior to the subdivision (b: any integer), and i denotes the number of stippled cubes to stipple at each subdivision of a non-stippled hypercube. Since i is greater than zero, D^d is less than d; that is,

$$D^1 < 1, \quad D^2 < 2, \quad D^3 < 3. \quad (8)$$

Moreover, size distributions with a negative fractal dimension have never been recognized for fragmented objects. These are important constraints that will be used in later discussion.

IMPLICATIONS FOR THE ORIGIN OF PSEUDOTACHYLYTES

The size distribution gives a constraint on the relative abundance of clasts having different range of size. This relative abundance is determined by the fractal dimension in the case of power laws. We shall now use this constraint to estimate the fraction of ultrafine clasts from the measured fractal dimension for coarse clasts. Basic premises here are that the shape of clasts does not change significantly with size and that the same type of power law holds for ultrafine submicroscopic clasts, but with unknown fractal dimension, D_X (Fig. 5).

The size distributions for fine and coarse clasts in Fig. 5 can be expressed, respectively, as:

$$N/N' = (r/r')^{-D_X} \quad (9)$$

$$N/N' = (r/r')^{-D}. \quad (10)$$

Here N is the cumulative number of objects whose characteristic length is greater than r, and N' and r' are the cumulative number and the size at the inflection point for the size distributions. Because the area occupied by a particle with size, r, is kr^2, where k is a shape factor, the total area occupied by all clasts with sizes ranging from r' to r_{max} is given by:

$$A = (kN'Dr'^D)(r_{max}^{2-D} - r'^{2-D})/(2 - D). \quad (11)$$

An identical form of equation holds for the area, occupied by ultrafine clasts, A_X.

The relative abundance of coarse and fine clasts can thus be evaluated, so one can test whether the amount of matrix of the pseudotachylyte is consistent with the predicted amount of fine clasts from the size distribution. In the evaluation here we used the values $D = 1.5$, $r' = 5\,\mu$m and $r_{max} = 2000\,\mu$m based on the data for

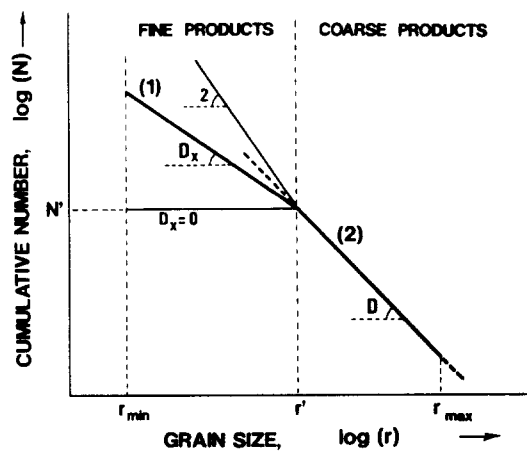

Fig. 5. Measured size distribution for clasts in pseudotachylytes with fractal dimension, D, and the presumed size distribution for ultrafine, submicroscopic clasts with unknown fractal dimension, D_X. r_{min} and r_{max} are the assumed minimum size and the maximum measured size of clasts, respectively.

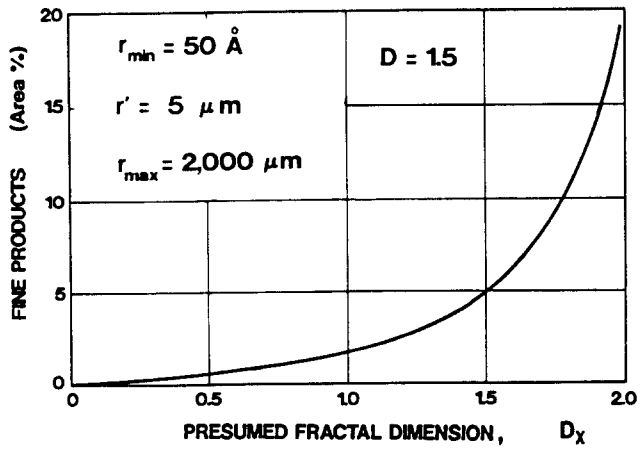

Fig. 6. Predicted area (percent) occupied by ultrafine products, for various values of the unknown fractal dimension, D_X. The values of parameters are inset in the upper-left corner.

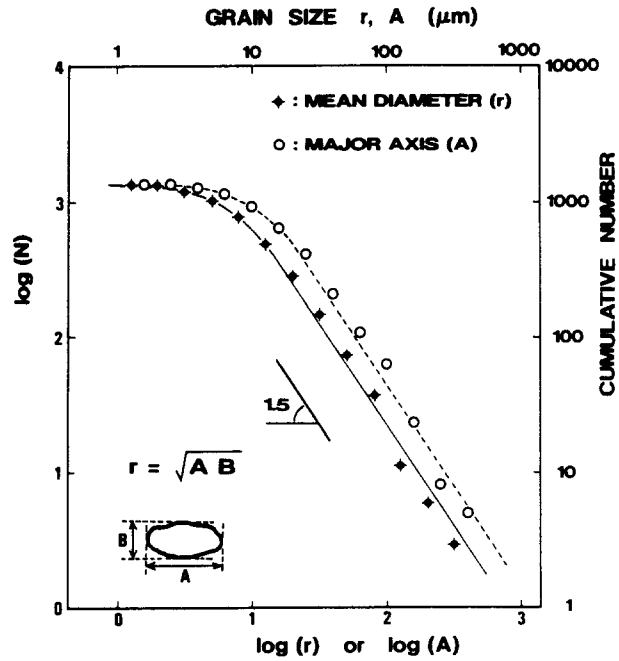

Fig. 7. Size distribution of finer clasts contained in the felsic pseudotachylyte (specimen No. 1) from the Musgrave Range, central Australia (for notations see caption of Fig. 2). The measurements were made on the same thin section as that used for the measurements in Fig. 2, using more enlarged photomicrographs. The minimum detectable size on the photomicrographs were about 1–2 μm.

coarse clasts in Fig. 2. The minimum size of clasts was assumed arbitrarily as 50 Å, a few times larger than the unit cell of common minerals, and the fractal dimension, D_X, could vary from 0 up to nearly 2.

The result predicts that the total area for fine clasts is in most cases less than several percent (Fig. 6). The area rapidly increases with increasing D_X when D_X approaches 2, but does not exceed 20%. As will be discussed later, the case for $D = 2$ over wide size ranges is quite unlikely, and hence the area for fine products, expected from the clast-size distribution, is perhaps on the order of several percent. The extrapolation of the measured size distribution towards fine sizes yields an area for fine clasts of about 5% (Fig. 6).

The actual area of the ultrafine-grained matrix of the same specimen is measured as 60%, by using a point-counting technique on the same photomicrographs. This is one order of magnitude greater than the predicted value from the size distribution. So on this basis, a major portion of the matrix cannot be regarded as being of the crush origin.

A critical point regarding the above estimation is the size distribution of fine-grained clasts. Hence we have measured the size distribution of finer grains on the same specimen shown in Fig. 2, using more enlarged photomicrographs (Fig. 7). The results are somewhat surprising, because the cumulative-number vs clast-size curves becomes flattened towards smaller grain sizes in the small size regimes; the size distribution for sizes greater than about 10–20 μm are nearly identical to those shown in Fig. 2. The flattening of the curves means that clasts smaller than about 5 μm are not common in pseudotachylytes. In our opinion, this clearly denies the crush origin of the matrix of the pseudotachylyte from the Musgrave Range, because if the ultrafine-grained matrix of pseudotachylytes had formed by severe crushing, the crushing and fragmentation must have jumped the size range of 1–5 μm to form the ultrafine matrix. This, however, seems to be physically unreasonable. We believe that the lack of fine clasts demonstrated in Fig. 7 is due to nearly complete melting of fine clasts, since corroded margins of clasts are very common in the pseudotachylyte from the Musgrave Range (e.g. Fig. 1b).

CONCLUSIONS AND DISCUSSIONS

The major results of the present work are summarized as follows.

(1) The clasts of various sizes contained in a pseudotachylyte from the Musgrave Ranges, central Australia, obey a power-law size distribution with a fractal dimension of 1.5 (Fig. 2).

(2) A new method for estimating the fraction of ultrafine clasts from the power-law size distribution of measured clasts is proposed. The estimated amount of ultrafine clasts is smaller than the true area of the fine-grained matrix by about one order of magnitude (Fig. 6), which suggests that the matrix of the pseudotachylyte was not formed by progressive fragmentation (crushing).

(3) Clasts in the size range of 1–5 μm are almost absent from the pseudotachylyte veins from the Musgrave Range (Fig. 7). This further refutes a crush origin for the matrix of the pseudotachylyte, because crushing and fragmentation are most unlikely to jump a certain range of sizes, and then form even finer-grained crush products.

Although the predicted amount of fine clasts (Fig. 6) is not particularly small when D is close to 2, the size distribution with $D_X \simeq 2$ is quite unlikely to hold over the entire range from 50 Å to 5 μm in view of the

properties of the power-law size distribution summarized in a previous section. The fractal dimension of 2 corresponds to the case in which the number of stippled cubes, i, in equation (7) is zero. In other words, the case for $D = 2$ implies lack of size distribution, and the breakdown of the power-law distribution. Thus a fractal dimension close to 2 is not expected to hold over a wide range of sizes. Moreover, a lower bound in the grain-size reduction is most likely to exist, owing to the rapid increase in the total surface area upon further grain-size refinement. Below this limiting size, there is no increase in the cumulative number of fragments and the fractal dimension sharply reduces to zero. Such a lower bound in the clast-size refinement further reduces the predicted amount of ultrafine clasts to below that shown in Fig. 6. Hence nearly one-order-of-magnitude or even more difference in the predicted and observed amounts of fine-grained matrix of the pseudotachylyte (result 2 above) is probably real.

The method proposed here provides a new way of looking at pseudotachylytes, and we hope that various pseudotachylyte veins from other regions will be examined by this technique. In applying the technique, however, one must be careful about the interpretation, when pseudotachylyte veins occur near a distinct cataclastic fault zone. This is because the fault zone could have acted as the reservoir for ultrafine-grained clasts which could have been fluidized and transported for some distance. For precise arguments in such cases, the analysis of clast-size distribution must be carried out over the entire cataclastic fault zone. In order to avoid such an overwhelming difficulty, we selected pseudotachylyte veins from a thrust without a distinct cataclastic fault zone. The lack of a cataclastic fault zone in a massive pseudotachylyte zone may have an important bearing on the pseudotachylyte problem, but this will be discussed elsewhere.

Results (2) and (3) above, combined with textural evidence such as the development of microlites and corroded structures (Fig. 1b), strongly suggest the melt origin for the matrix of pseudotachylyte from the Musgrave Range, central Australia. A more comprehensive argument about the origin of pseudotachylytes will be made elsewhere.

Acknowledgements—We sincerely thank Alfredo Camachol of the Northern Territory Geological Survey, Australia, for taking one of us (T. Shimamoto) to the impressive outcrops of pseudotachylyte in the Musgrave Ranges. We also thank M. Kitamura (Kyoto University) for many stimulative discussions and J. G. Spray (University of New Brunswick) and G. E. Lloyd (Leeds University) for their careful reviews of the manuscript.

REFERENCES

Clough, C. T. 1888. *The Geology of the Cheviot Hills*. England and Wales Geological Survey Memoirs.

Fujiwara, A., Kamimoto, G. & Tsukamoto, A. 1977. Destruction of basaltic bodies by high-velocity impact. *Icarus* **31**, 277–288.

Gaudin, A. M. 1926. An investigation of crushing phenomena. *Trans. Am. Inst. Mining Metall. Petrol. Engrs* **73**, 253–316.

Hanks, T. C. & Raleigh, C. B. (editors) 1980. *Proceedings of the Symposium, "Stress in the Lithosphere". J. geophys. Res.* **85**, 6083–6435.

Hartmann, W. K. 1969. Terrestrial, lunar, and interplanetary rock fragmentation. *Icarus* **10**, 201–213.

Maddock, R. H. 1983. Melt origin of fault-generated pseudotachylytes demonstrated by textures. *Geology* **11**, 105–108.

Mandelbrot, B. B. 1982. *The Fractal Geometry of Nature*. W. H. Freeman, San Francisco.

Matsushita, M. 1985. Fractal viewpoint of fracture and accretion. *J. Phys. Soc. Jap.* **54**, 857–860.

Moore, A. C. & Goode, A. D. T. 1978. Petrography and origin of granulite-facies rocks in the western Musgrave Block, central Australia. *J. geol. Soc. Aust.* **25**, 341–358.

Nagahama, H. 1991. Fracturing in the solid earth. *Sci. Rep. Tohoku Univ.* (Geol.) **61**, 103–126.

Okamoto, Y. & Kitamura, M. 1990. A mineralogical study of psuedotachylytes from Scotland.(In Japanese.)(*Abst.*) Annual Meeting of Mineralogical Society of Japan, 47.

Philpotts, A. R. 1964. Origin of pseudotachylytes. *Am. J. Sci.* **262**, 1008–1035.

Sammis, C. G., Osborne, R. H., Anderson, J. L., Banerdt, M. & White, P. 1986. Self-similar cataclasis in the formation of fault gouge. *Pure & Appl. Geophys.* **124**, 53–78.

Schroeder, M. 1991. *Fractals, Chaos, Power Laws*. W. H. Freeman, San Francisco.

Schuhmann, R., Jr. 1960. Energy input and size distribution in comminution. *Trans. Am. Inst. Mining Metall. Petrol. Engrs* **217**, 22–25.

Shand, S. J. 1916. The pseudotachylyte of Parijs (Orange Free State) and its relation to 'trap-shotten' gneiss and 'flinty crush' rock. *Q. Jl geol. Soc. Lond.* **72**, 198–221.

Shimamoto, T. & Nagahama, H. 1991. The origin of pseudotachylytes and the state-of-stress problem. (In Japanese.) *Earth Monthly* **13**, 416–427.

Sibson, R. H. 1975. Generation of pseudotachylyte by ancient seismic faulting. *Geophys. J. R. astr. Soc.* **43**, 775–794.

Takeuchi, H. & Mizutani, H. 1968. Relation between earthquake occurrence and brittle fracture. (In Japanese.) *Kagaku (Science), Iwanami Shoten. Tokyo* **38**, 622–624.

Toyoshima, T. 1990. Pseudotachylites from the Main Zone of the Hidaka metamorphic belt, Hokkaido, northern Japan. *J. metamorph. Geol.* **8**, 507–523.

Turcotte, D. L. 1986. Fractals and fragmentation. *J. geophys. Res.* **91**, 1921–1926.

Webb, A. W. 1985. Geochronology of the Musgrave block. *Mineral Resourc. Rev., Dept Mines & Energy, Aust.* **155**, 23–37.

Weiss, L. E. & Wenk, H.-R. 1983. Experimentally produced pseudotachylyte-like veins in gabbro. *Tectonophysics* **96**, 299–310.

Wenk, H.-R. 1978. Are pseudotachylites products of fracture or fusion? *Geology* **6**, 507–511.